

Dilatancy and friction in sheared granular media

Frederic Lacombe, Stefano Zapperi and Hans J. Herrmann
PMMH-ESPCI, 10 rue Vauquelin, 75231 Paris Cedex 05, France

We introduce a simple model to describe the frictional properties of granular media under shear. We model the friction force in terms of the horizontal velocity \dot{x} and the vertical position z of the slider, interpreting z as a constitutive variable characterizing the contact. Dilatancy is shown to play an essential role in the dynamics, inducing a stick-slip instability at low velocity. We compute the phase diagram, analyze numerically the model for a wide range of parameters and compare our results with experiments on dry and wet granular media, obtaining a good agreement. In particular, we reproduce the hysteretic velocity dependence of the frictional force.

I. INTRODUCTION

Problems related to interfacial friction are very important from a practical and conceptual point of view [1], and in spite of its wide domain of application sliding friction is still not completely understood. In order to construct efficient machines in engineering science, or to understand geophysical events like earthquakes, it is necessary to understand several aspects of friction dynamics. Beside usual solid-solid contacts, the sliding interface can be lubricated with molecular fluids or filled by a granular gauge, and the problem becomes strongly dependent on the internal dynamics of the material itself. In experiments on lubricated surfaces with thin layers of molecular fluids the friction force depends on the thermodynamic phase of the lubricant, which depends on its turn on the shear stress [2]. The friction force is thus directly related to the microscopic dynamics of the system and a description of sliding friction cannot be achieved without a good microscopic understanding of the problem. Understanding the frictional properties of granular matter turns out to be an even harder task, since basic problems like stress propagation in a static packing remain largely unsolved due to the disordered nature of the stress repartition inside the medium. Moreover, when a granular medium is sheared, it reorganizes modifying the geometrical disorder. The microscopic arrangement of the grains and their compaction have an important effect on the friction since, in order to deform the medium one has to overcome several geometrical constraints.

The understanding of sheared granular media has recently advanced thanks to experiments [3–6] and numerical studies [7–9]. The response to an external shear stress can be characterized by the dilatancy, which measures the modification of the compaction of the granular medium during the flow [7]. We note that in both lubricated and granular interfaces the friction force has a dynamical origin. Since a sheared material modifies its own internal state fluidizing or changing structure, a natural approach to the problem is to describe phenomenologically this change of state and to relate it to the macroscopic friction force. As we discussed previously, a complete theoretical description of sheared granular media is still not available, so that the analysis should strongly rely on experimental data.

Recent experiments [3], focusing on the stick-slip instability induced by friction in sheared granular layers, helped to elucidate the role of compaction and the microscopic origin of slip events. In particular, accurate measurement of the friction force and of the horizontal and vertical positions of the slider [4] have permitted to emphasize the connections between dilatancy and friction. The apparatus used was composed by a slider dragged at constant velocity by a spring whose elongation measured the applied shear stress. The surface of the slider was roughened in order to avoid slip at the surface of the medium and so that friction would crucially depend on the internal structure of the medium. At low velocity, a stick slip instability was observed and related to the modification in the granular compaction.

Friction of granular layers has been mainly studied in the framework of geophysical research [5,10] using rate and state constitutive equations [11–15] where the friction force is a function of an auxiliary variable describing the state of the interface. In this approach, one assumes that the microscopic events causing the movement of the slider are self-averaging and neglects the fluctuations. The quantities used in the constitutive equations are thus mean field-like. This assumption should be valid for sliding friction experiments on granular materials, where the size of the grain is much smaller than the length of the slider, so that the variables used in the model (velocity, displacement or friction force), are well defined macroscopical quantities.

The constitutive variable, related to the microscopic dynamics of the system, describes the dynamical history of the interface. In the case of solid-solid interfaces [16] this variable was associated with the age of the contacts and described two opposite effects: the age of the contact increases the static friction force and the displacement of the slider renews the interface continuously so that the friction force decreases with velocity. Lubricated systems have been approached similarly using the rate of fluidization as a constitutive variable [17,18] which captures two different effects. On one hand the confinement of the thin fluid layer induces a glassy transition resulting in a large static friction

force. On the other hand an applied shear stress increases the temperature of the medium, favoring fluidization, thus reducing the friction force, which crucially depends on the ratio between the strength of the two effects.

In the case of granular media, a parameter suitable to characterize the frictional behavior is the compaction of the layers or the height of the slider which can be measured experimentally. Also in this case we can identify the competition between two opposite effects: the velocity of the slider keeps the layer dilated, lowering the friction force, and the weight of the slider induces recompaction. In this paper we present a model which includes these two effects in the framework of rate and state constitutive equations to describe typical effects like the stick-slip instability or the force-velocity hysteretic loop.

In Sec. II we concentrate on the description of the model, in Sec. III we describe the main results obtained by numerical integration of the model, in Sec. IV we present a stability analysis and the phase diagram. Finally, Sec. V presents a discussion and a summary of our results.

II. THE MODEL

Here we write rate and state constitutive equations in order to describe the frictional properties of granular media. The dynamics of the sliding plate is described by two constitutive equations. The first one is simply the equation of motion for the slider block driven by a spring of stiffness k and submitted to a frictional force, which depends on velocity and dilatancy. The second equation is the evolution law for an auxiliary variable characterizing the dilatancy, which we will identify with the vertical position of the slider. This model could in principle be applied to geophysical situations, although in that case instead of a single elastic constant k , strain is mediated via the material bulk elasticity.

The frictional properties of a granular medium depend explicitly on its density: a dense granular medium submitted to a tangential stress tends to dilate, *i.e.* to modify the granular packing and thus the friction force. It is not simple to measure granular density especially for non homogeneous systems, but global changes can be characterized by the vertical position of the sliding plate, which is thus an excellent candidate to describe the state of the system. Therefore, in agreement with Ref. [4], we write the equation of motion for the slider block as

$$m\ddot{x} = k(Vt - x) - F(z, \dot{x}), \quad (1)$$

where m is the mass of the sliding plate, x its position, k the spring constant, V the drag velocity, and $F(z, \dot{x})$ the friction force depending on the velocity \dot{x} and on the height of the plate z .

If the slider is at rest, we need to apply a minimal constant force F_0 in order for it to move. When the force exceeds F_0 , the slider moves and dilation will occur, reducing the friction. When the layer is fully dilated the friction reduces to $F_d < F_0$. We assume that the friction force is velocity dependent when the layer is partially dilated ($z < z_m$), and becomes independent on velocity in the stationary state, when the granular medium is fully dilated ($z = z_m$).

In summary (in the case $\dot{x} > 0$), we write the friction force as

$$F(z, \dot{x}) = F_d - \beta \frac{z - z_m}{R} - \nu \dot{x} \frac{z - z_m}{R}. \quad (2)$$

The first two terms in Eq. (2) give the friction force at rest ($\dot{x} = 0$) as function of z . In the fully expanded phase ($z = z_m$), the friction term is $F = F_d < F_0$, while in the compacted phase $F_0 = F_d + \beta z_m / R$ ($z = 0$). The velocity dependence is linear, mediated by the factor $z - z_m$ which vanishes when the bed is fully dilated. These equations should be compared with those presented in Ref. [4], where the second term in Eq. (2) is not present.

In Eq. (2) $F(z, \dot{x})$ depends explicitly on z , which describes the vertical displacement of the slider. In order to complete the description of the dynamics, we must specify the evolution equation for z . We write the law controlling the dilation of the granular medium during shear as

$$\dot{z} = -\frac{z}{\eta} - \dot{x} \frac{z - z_m}{R}. \quad (3)$$

In Eq. (3) the second term dilates the support and can be seen as the response of the granular medium to the external tangential stress: when submitted to a shear rate \dot{x} , the medium dilates and z increases. The factor $(z - z_m)$ reduces to zero when the bed is fully dilated and z_m can be identified with the maximal height.

The first term allows for recompaction under the slider weight: in the case $\dot{x} = 0$ the plate falls exponentially fast. At high velocity this term will not perturb significantly the system and the dynamics will be stationary. We are interested in the small velocity limit: Eqs. (2,3) will display an instability below a critical drag velocity V_c , as we will show in Sec. IV.

It is useful to rewrite the system of equations in terms of dimensionless variables

$$\begin{aligned}\tilde{t} &= t \frac{k}{\nu}, & \tilde{\eta} &= \eta \frac{k}{\nu}, & \tilde{x} &= \frac{x}{R}, & \tilde{z} &= \frac{z}{R}, & \tilde{z}_m &= \frac{z_m}{R}, \\ \tilde{m} &= m \frac{k}{\nu^2}, & \tilde{V} &= V \frac{\nu}{Rk}, & \tilde{v} &= v \frac{\nu}{Rk}, & \tilde{F}_d &= \frac{F_d}{Rk}, & \tilde{\beta} &= \frac{\beta}{Rk}.\end{aligned}$$

Defining $\tilde{l} = \tilde{V}\tilde{t} - \tilde{x} - \tilde{F}_d$, the system becomes

$$\dot{\tilde{l}} = \tilde{V} - \tilde{v}, \tag{4}$$

$$\tilde{m}\dot{\tilde{v}} = \tilde{l} + (\tilde{z} - \tilde{z}_m)(\tilde{v} + \tilde{\beta}), \tag{5}$$

$$\dot{\tilde{z}} = -\frac{\tilde{z}}{\tilde{\eta}} - (\tilde{z} - \tilde{z}_m)\tilde{v}. \tag{6}$$

Assuming that these equation are valid for $\dot{x} > 0$, we can analyze them for different spring constants, velocity.

III. NUMERICAL SIMULATIONS

We numerically solve the model (Eqs. (4-6)) using the fourth order Runge-Kutta method and assuming that the slider plate sticks when its velocity is zero. We concentrate our analysis on two sets of parameters. The first set corresponds to experiments carried out with a dry granular medium. We compute the typical force-velocity diagram in order to fix the parameters. Then using the same parameters we test the validity of our model calculating other quantities such as the slider velocity during a slip event, the spring elongation or the vertical displacement.

A second set of parameters is used to model wet granular media. We recover the instability at low velocity and low spring force and study the evolution of dilatancy and spring elongation before reaching the steady-state.

A. Dry granular media

Dry granular media exhibit stick-slip instabilities for relatively high velocities and it is difficult to achieve complete vertical displacement of the slider. For this reason the steady sliding regime has not been studied in detail in experiments. In order to quantitatively test our model we adjust the parameters to fit the experimental results. We present in Fig. 1 the force-velocity curve during slip comparing the experimental data from Ref. [3] with the result of the integration of the model. The parameters used are given in the caption. The model is able to accurately describe the first part of the hysteretic loop (when the velocity increases), but slight deviations appear for small velocities for which also the experimental uncertainties are larger.

We numerically integrate the model using the previously obtained parameters, varying the spring constant and the driving velocity. For slow velocity and a small spring constant the system exhibits typical stick-slip dynamics. Fig. 2 shows the evolution of the variables of the model in this case: the first plot (Fig. 2(a)) shows the variation of the spring length which decreases abruptly at a regular frequency, when the horizontal plate position increases (Fig. 2(b)). Fig. 2(c) represents the velocity of the plate which is followed by an increase of the vertical position of the plate (Fig. 2(d)). We show in Fig. 3 a more detailed study of the slider velocity during a slip event. Near the transition between the stick-slip and the steady sliding regime the slider velocity appears to be almost independent on the driving velocity, in agreement with experiments. The stick-slip instability of the model is ruled by Eqs. (4-6) and we present in Sec. IV the dynamical phase diagram computed by a linear stability analysis. When the slider is driven slowly the energy injected into the granular medium cannot keep the layers dilated and the motion stops after a short change in the horizontal position (slip event).

If we increase V or k , the energy induced by the shear is sufficient to maintain the granular layer dilated and the system evolves to a steady sliding state (cf. Fig. 4), which is stable with respect to small perturbations. This stationary state, corresponds to a stable fixed point of Eqs. (4-6) (see Sec. IV). If the drag velocity is very large the steady sliding state becomes unstable due to inertial effects ($m \neq 0$) and the slider oscillates harmonically with frequency $\omega = \sqrt{k/m}$. This effect was experimentally observed in Ref. [3]. We have plotted the result in Fig. 5 for two different perturbations, in order to show that the amplitude of the cycle depends on the strength of the perturbation.

A typical measurement performed in the framework of geophysical research [5,10], is the variation of the friction force with respect to a rapid change of the driving velocity. We have simulated this effect, and we show the result

in Fig. 6. An increase of the driving velocity is followed by an increase of the friction force which then relaxes to a smaller value.

The phase diagram corresponding to the three different dynamical behaviors can be calculated analytically. We present the result in Sec. IV, where we study the linear stability of the model.

B. Wet granular media

The analysis performed in Sec. III A can be repeated for wet granular materials. The dynamics in this case is more stable and the stick-slip regime is more difficult to obtain experimentally, since the instability occurs at very slow velocity. In the wet case, the presence of water changes the dynamics of the grains. Under shear, grains reorganize submitted to the fluid viscosity but here we neglect the small hydrodynamic effects and consider only the grain dynamics with suitable parameters. Using the new class of parameters, we solve numerically Eqs. (4-6) and identify two regimes: steady sliding at high V and stick-slip instability otherwise (see Sec. IV for more details). In Fig. 7 we show a typical plot of the different quantities in the stick-slip regime. The period of the oscillations is bigger than in the dry case, and the fluctuations of the elongation smaller. One of the main difference with the dry case is the value of η which governs the relaxation process and which is greater in the wet case as an effect of immersion. In Fig. 8 we show the steady state found at high velocity. It is interesting to remark that this behavior can be perfectly recovered with a simplified model, presented in Ref. [4], which however does not give rise to stick-slip instabilities. We will show in the next section that our model is equivalent to the model of Ref. [4] for a given range of parameters. Fig. 9 represents the integration in the case $\beta > \frac{\nu R}{\eta}$ (the importance of the value of β will be highlighted in Sec. IV).

Ref. [4] also reported an experiment in which the slider was stopped abruptly, but the applied stress was not released. Under these conditions, the medium does not recompactify towards the initial state but remains dilated in an intermediate state. This feature cannot be captured by our model, since the evolution of z does not explicitly depend on the applied stress but only on the horizontal velocity. In order to describe this effect, we modify Eq. (3) in order to explicitly include a stress dependence in the evolution of the dilatancy

$$\dot{z} = -\frac{z - AF_{ext}}{\eta} - \dot{x} \frac{z - z_m}{R}, \quad (7)$$

where $F_{ext} = k(Vt - x)$ is the applied force and A is a constant. The behavior of this model is similar to the simpler model introduced in Section II, but the zero velocity fixed point explicitly depend on the applied stress (i.e. $z^* = AF_{ext}$). Fig. 10 shows the solution of the model compared with the experiment of Ref. [4].

IV. LINEAR STABILITY

The simple form of Eqs. (4-6) allows us to study analytically the linear stability of the system. We first concentrate on the inertial case and describe the main results about the dynamics of our problem (fixed point, critical curve). Next we discuss the origin of the instability and the connections with other models. Finally we investigate the nature of the bifurcation.

A. Inertial case

All the numerical results presented above have been obtained including inertial effects. The system of Eqs.(4-6) has a simple fixed point

$$l_c = z_m \frac{V\nu + \beta}{Rk + \eta V k}, \quad v_c = V, \quad z_c = z_m \frac{\eta V}{R + \eta V}. \quad (8)$$

We see that z_c tends to z_m when V tends to infinity, in agreement with experimental result. The critical line can also be computed explicitly in the framework of linear stability analysis. We skip the details of the calculations and just give the result

$$k^* = -\frac{z_m \nu^2 \eta R^2 - z_m \nu \eta^2 R \beta + m R^3 \nu - m R^2 \eta \beta + 2m R^2 \eta V \nu - 2m R \eta^2 V \beta + m R \eta^2 V^2 \nu - V^2 m \eta^3 \beta}{\nu \eta^2 R^2 (R + \eta V)}. \quad (9)$$

Fig. 11 and Fig. 12 show the phase diagram in the k, V plane for the parameters used previously (in Sec. III A and Sec. III B). For both dry and wet granular layers we recover the stick-slip regime at sufficiently small k and V . In the dry case the critical velocity is higher than in the wet case and we can also identify the inertial regime on the right hand side of the phase diagram (see Fig. 11).

B. Non inertial case

If we are interested only in low velocity displacements, the dynamical bifurcation line can be easily computed neglecting the mass of the slider

$$k^* = \left(\frac{\beta}{R} - \frac{\nu}{\eta}\right) \left(\frac{z_m}{R + \eta V}\right). \quad (10)$$

Also in this case the dynamics is unstable for k below the critical line, but there is no inertial regime. We have no experimental results to compare with this relation which links all the relevant parameter of the model.

Due to the simplicity of the non inertial case, we can write our system in the traditional form of a Hopf bifurcation [19], and calculate the coefficient which determines the nature of the transition. Without the inertial term this coefficient simply reduces to zero and therefore we have no information about the nature (super or subcritical) of the transition without pushing the calculation to higher orders or including inertia. However, the calculation is particularly complex so we only analyze the problem numerically (see Sec. IVD).

C. Dynamical friction force

The stick-slip instability is due to the dependence of the friction coefficient on the velocity. Here we compute the friction force corresponding to the fixed point and show that the sign of $\beta/R - \nu/\eta$ plays an important role to determine the presence of an instability. In the steady state the friction force is given by

$$F_c = F_d + z_m \frac{1}{R + \eta V} (\beta + \nu V). \quad (11)$$

For sufficiently high V , F_c does not depend on V , in agreement with experiments, but for relatively small velocities $F_c(V)$ depends on V . The first derivative of the force is

$$\frac{dF_c(V)}{dV} = -\frac{R\eta}{R + \eta V} \left(\frac{\beta}{R} - \frac{\nu}{\eta}\right). \quad (12)$$

We can thus identify three cases:

- if $(\beta/R - \nu/\eta)$ is positive then there is a k verifying Eq. (10) and below this k the system is unstable (the derivative in V of $F_c(V)$ is negative *i.e.* $F_c(V)$ decreases with V).
- if $(\beta/R - \nu/\eta)$ is negative the system is always stable (k cannot be negative).
- if $(\beta/R - \nu/\eta = 0)$ then $F_c(V)$ does not depend on V . In this case the system is stable and we can write the friction force as

$$F(z, \dot{x}) = F_s + \nu \dot{z}, \quad (13)$$

with $F_s = F_d + \nu z_m/\eta$. The form given in Eq. (13) for the friction force, together with Eq. (3), implies a friction coefficient independent on V and a stable steady state for all the values of the parameters. In the limit $\eta \gg 1$, and assuming Eq. (13), β tends to 0 and the dilatancy rate is given by

$$\dot{z} = -\dot{x} \frac{z - z_m}{R}, \quad (14)$$

which reproduces the model of Ref. [4].

D. Nature of the bifurcation line

The calculation in the non inertial case does not allow us to know the exact nature of the transition. Thus we investigate this problem numerically: the system is perturbed near its fixed point in the vertical position with different displacements ($0.4\mu m - 0.002\mu m$). Two final states can be obtained depending on the position in the phase diagram: the system can evolve to the steady state or be driven to the stick-slip cycle. In an intermediate zone depending on the strength of the perturbation, the system can recover both the fixed point or the stick-slip regime.

We identify three regimes, the first corresponds to the stick-slip regime where, independently on the amplitude of the perturbation the system falls into a periodic cycle. In the second regime, associated with high driving velocity, the system evolves to the stable fixed point. In the third intermediate regime, the final state depends on the initial perturbation: if the perturbation is sufficiently large the system falls into a periodic regime, while if the perturbation is weak it evolves towards the fixed point. The transition between the two regimes is discontinuous (*i.e* subcritical). Fig. 13 shows the amplitude of the oscillations as a function of the driving velocity. It would be interesting to check experimentally the hysteretic nature of the bifurcation line.

The presence of an hysteretic transition line could be related to an underlying first-order phase transition in the layer density induced by the applied stress. Recently [20], analyzing the results of photoelastic disks in a two dimensional shear cell, it has been argued that the density of a the granular packing would be the order parameter of a second order phase transition induced by shear. It would be interesting to relate the different experimental phase transitions through a suitable microscopic model.

V. DISCUSSION AND OPEN PROBLEMS

We have introduced a model to describe the friction force of a sheared granular medium, treating explicitly the dilatancy during the slip, in the framework of rate and state constitutive equations. This approach allows us to include in the description the effect of the movement of the grains and the dependence of the friction coefficient on the dynamics of the layer. The variables used are mean-field like, since they represent macroscopic quantities like the position or the velocity but they are sufficient to describe phenomenologically the system. We have integrated the model for two sets of parameters, in order to make quantitative predictions for two different experimental configurations corresponding to dry and wet granular media.

The results are in good agreement with experiments. In particular, we recover the hysteretic dependence of the friction force on velocity and obtain a good fit to the experimental data recorded in dry granular media. The effect of the weight of the slider plate is included in the model and allows us to recover a stick-slip instability at low velocity. The physical origin of the instability is then directly related to the recompaction of the material under normal stress. The dynamical phase diagram is calculated analytically both in the inertial and non inertial cases and inertia is found to change only the high velocity part of this diagram. The equations used to model the dependence of the friction law on the external parameters include explicitly the effect of recompaction in the evolution of the vertical slider position.

The use of constitutive equations to model the friction force on complex interfaces is the simplest way to obtain quantitative results on the dynamics of the system. This approach provides good results in various fields, from geophysics or to nanotribology. In order to include the dynamics (or thermodynamics in the case of lubrication) of the material in the description, we need detailed informations about the material used. Our knowledge of sheared granular media is very poor due to the particulate and disordered nature of such materials and it is difficult to characterize the internal stress and strain rate. A precise description of the friction force for granular systems should include some information about the stress repartition inside the sheared material. This is a difficult problem which even for the simple case of a static pile cannot be solved completely. In the dynamical regime, the velocity depends on the precise nature of the contacts and on the friction force induced by them. Statistical models are needed to obtain a more complete macroscopic description based on the microscopic grain dynamics. In this respect, the analogy with phase transitions could be extremely fruitful.

Experiments on granular flow over a rough inclined plane display an interesting behavior [21,22], which is ruled by frictional properties. The dynamic stops abruptly when the drag force decreases and the system freezes with grains remaining in a static configuration. These phenomena can be related to the dependence of the friction force on the velocity of the grains: an increase of the friction force when the velocity of the layer decreases can produce an instability as in the system discussed here. It will be interesting to see if the methods discussed in this paper can be applied to this and other situations.

We thank J. S. Rice, and S. Roux for useful discussions and encouragements. We are grateful to J-C. Geminard for providing us with the data of his experiments and for interesting remarks. S. Z. is supported by EC TMR Research Network under contract ERBFMRXCT960062.

-
- [1] B.N.J. Persson, *Sliding Friction* (Springer, Berlin, 1998).
 - [2] M.L. Gee, P.M. McGuiggan and J.N. Israelachvili, *J. Chem. Phys.* **93**, 1895 (1990).
 - [3] S. Nasuno, A. Kudrolli, J.P. Gollub, *Phys. Rev. Lett.* **79**, 949 (1997); S. Nasuno, A. Kudrolli, A. Bak, J.P. Gollub, *Phys. Rev. E* **58**, 2161 (1998).
 - [4] J.C. Geminard, W. Losert, J.P. Gollub, *Phys. Rev. E* **59**, 5881 (1999).
 - [5] C. Marone, *Annu. Rev. Earth Planet. Sci.* **26**, 643 (1998).
 - [6] C.T. Veje, D.W. Howell and R.P. Behringer, *Phys. Rev. E* **59**, 739 (1999).
 - [7] P.A. Thompson and G.S. Grest, *Phys. Rev. Lett.* **67**, 1751 (1991).
 - [8] H.-J. Tillemans and H.J. Herrmann, *Physica A* **217**, 261 (1995).
 - [9] S. Schollman, *Phys. Rev. E* **59**, 889 (1999).
 - [10] P. Segall, J.R. Rice, *J. Geophys. Res.* **100**, **B11**, 22.155 (1995).
 - [11] J.H. Dietrich, *Pageoph.* **116**, 790 (1978).
 - [12] J.R. Rice, *Pageoph.* **121**, 443 (1983).
 - [13] J.-C. Gu, J.R. Rice, A.L. Ruina and S.T. Tse, *J. Mech. Phys. Solids* **32**, 167 (1984).
 - [14] J.R. Rice, A.L. Ruina, *J. Appl. Mech.* **50**, 343 (1983).
 - [15] A. Ruina, *J. Geophys. Res.* **88**, **B12**, 10.359 (1983).
 - [16] F. Helsot, T. Baumberger, B. Perrin, B. Caroli and C. Caroli, *Phys. Rev. E* **49**, 4973 (1994).
 - [17] A.A. Batista, J.M. Carlson, *Phys. Rev. E* **53**, 4153 (1996); *ibid.* **57**, 4986 (1998).
 - [18] B.N.J. Persson, *Phys. Rev. B* **55**, 8004 (1997).
 - [19] J. Guckenheimer and P. Holmes, *Nonlinear Oscillations, Dynamical Systems and Bifurcation of Vector Field* (Springer-Verlag, New York, 1983).
 - [20] D. Howell and R. P. Behringer, *Phys. Rev. Lett.* **82**, 5241 (1999).
 - [21] O. Pouliquen and N. Renault, *J. Phys. II France* **6**, 923 (1996).
 - [22] S. Douady and A. Daerr, in *Physic of dry granular media*, edited by H.J. Herrmann et al. (Kluwer Academic Publisher, Netherlands, 1998).

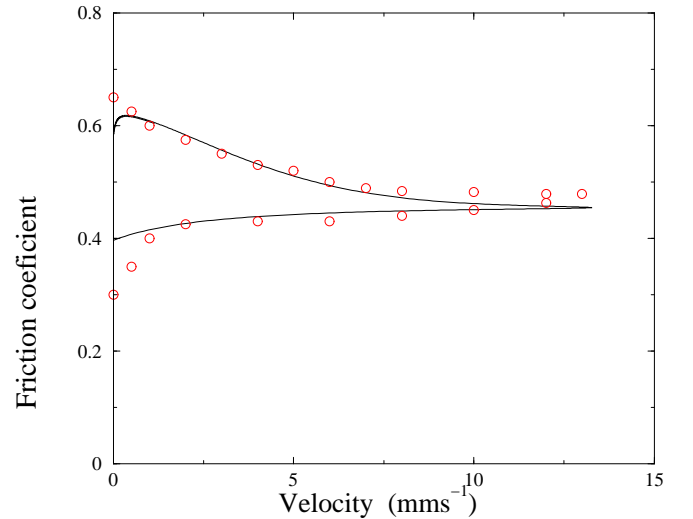


FIG. 1. Friction coefficient as a function of the slider velocity. The circles are the experimental data from Ref. [3] the line is the result of the model with parameters: $\nu = 90\text{Kgs}^{-1}$, $\eta = 0.1\text{s}$, $m = 11.3\text{g}$, $R = 8\mu\text{m}$, $z_m = 8\mu\text{m}$, $\beta = 3\frac{\nu R}{\eta}$, $k = 135\text{Nm}^{-1}$.

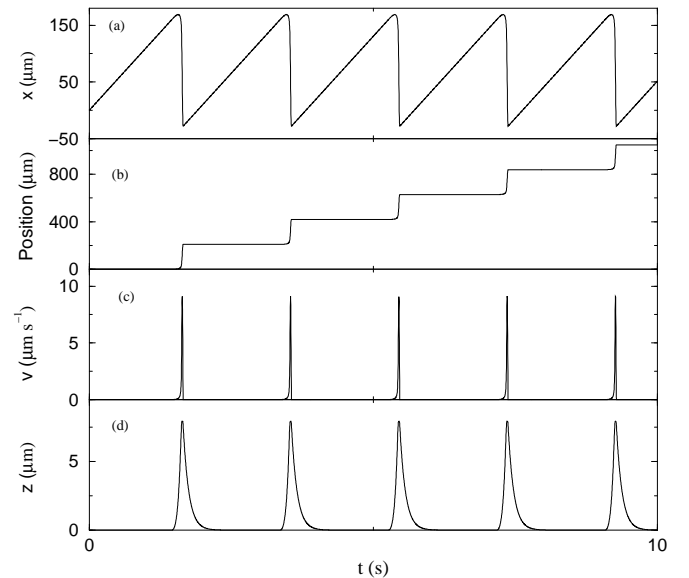


FIG. 2. Numerical calculation for dry granular media in the stick-slip regime. ($\nu = 90\text{Kgs}^{-1}$, $\eta = 0.1\text{s}$, $m = 10\text{g}$, $R = 8\mu\text{m}$, $z_m = 8\mu\text{m}$, $\beta = 3\frac{\nu R}{\eta}$, $V = 110\mu\text{ms}^{-1}$, $k = 135\text{Nm}^{-1}$). (a) spring elongation, (b) horizontal displacement, (c) slider velocity, (d) vertical displacement .

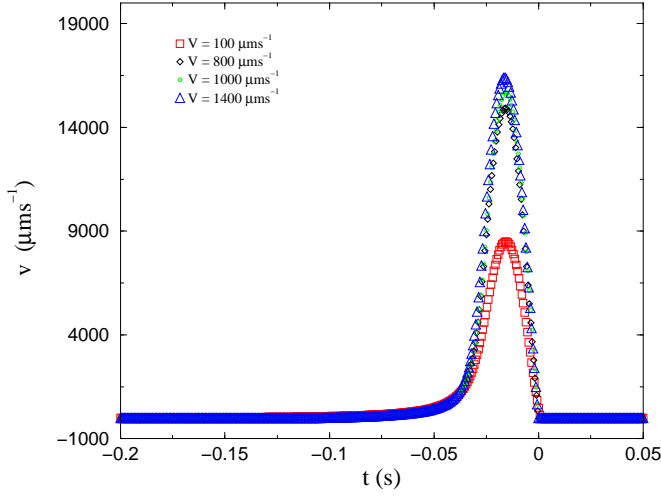


FIG. 3. Slider velocity for different loading velocities during a slip event. ($\nu = 90Kgs^{-1}$, $\eta = 0.1s$, $m = 10g$, $R = 8\mu m$, $z_m = 8\mu m$, $\beta = 3\frac{\nu R}{\eta}$, $k = 135Nm^{-1}$). Close to the transition point the maximum velocity is weakly dependent on the driving velocity.

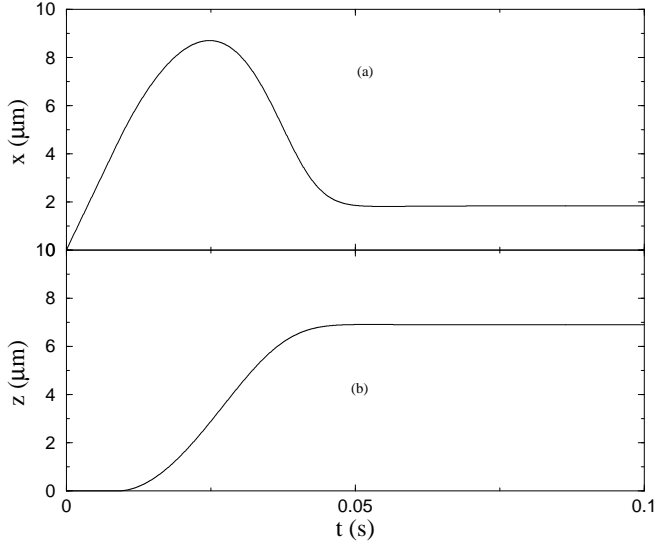


FIG. 4. Evolution to steady sliding state; numerical calculation for dry granular media. ($\nu = 90Kgs^{-1}$, $\eta = 0.1s$, $m = 10g$, $R = 8\mu m$, $z_m = 8\mu m$, $\beta = 3\frac{\nu R}{\eta}$, $V = 500\mu ms^{-1}$, $k = 5KNm^{-1}$). (a) spring elongation, (b) vertical position.

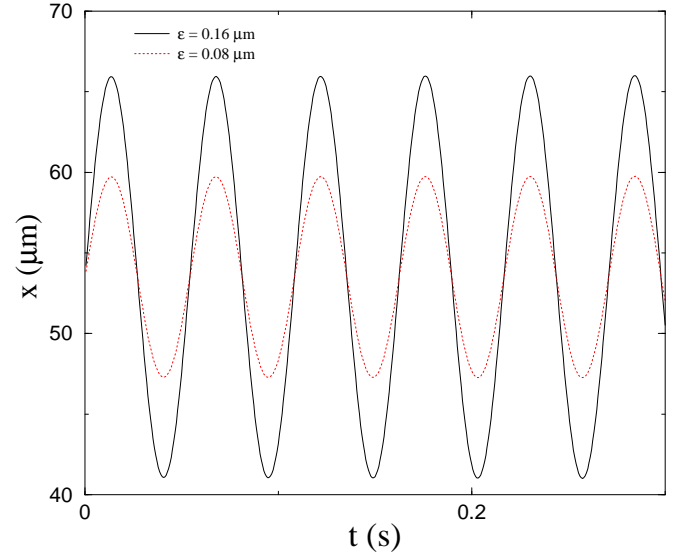


FIG. 5. Inertial oscillations. ($\nu = 90Kgs^{-1}$, $\eta = 0.1s$, $m = 10g$, $R = 8\mu m$, $z_m = 8\mu m$, $\beta = 3\frac{\nu R}{\eta}$, $V = 50mm s^{-1}$, $k = 135Nm^{-1}$). The amplitude of the cycle depends on the initial condition. Here $x_0 = x_c$, $v_0 = v_c$, $z_0 = z_c - \epsilon$, where ϵ is given in the legend, (x_c, v_c, z_c) is the fixed point.

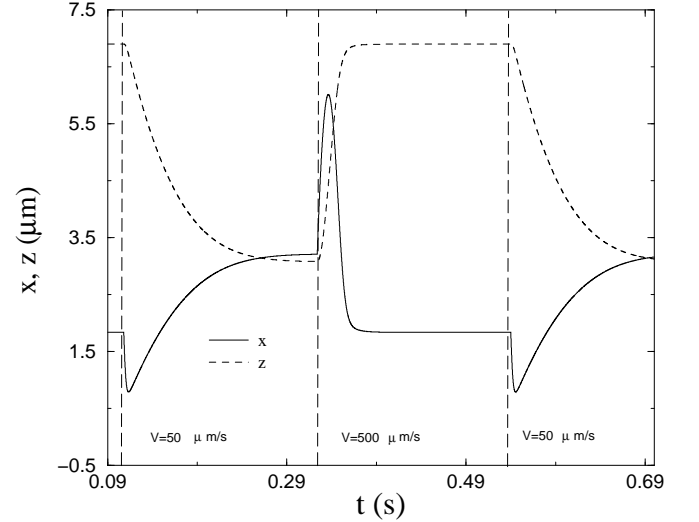


FIG. 6. The system is sheared at different constant velocities. We show the effect of the velocity change on the spring elongation and on dilatancy, see Ref. [15-17]. ($\nu = 90Kgs^{-1}$, $\eta = 0.1s$, $m = 10g$, $R = 8\mu m$, $z_m = 8\mu m$, $\beta = 3\frac{\nu R}{\eta}$, $V = 50 \text{ } 500\mu ms^{-1}$, $k = 5KNm^{-1}$).

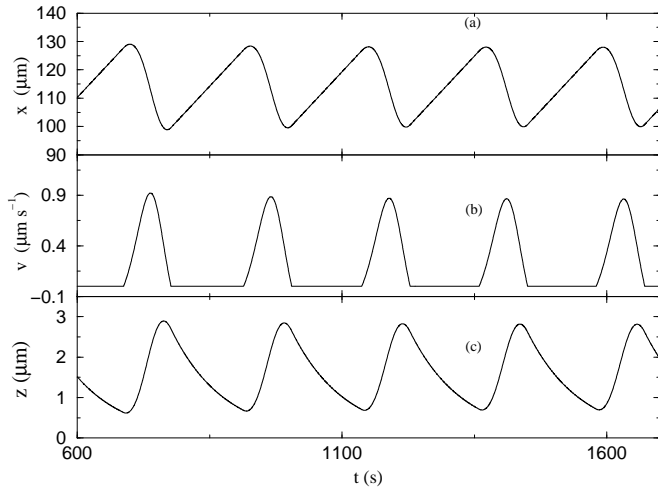


FIG. 7. Numerical calculation for wet granular media in the stick-slip regime. ($\nu = 10000Kgs^{-1}$, $\eta = 100s$, $m = 10g$, $R = 100\mu m$, $z_m = 10\mu m$, $\beta = 15\frac{\nu R}{\eta}$, $V = 0.2\mu ms^{-1}$, $k = 110Nm^{-1}$). (a) spring elongation, (b) plate velocity, (c) vertical position.

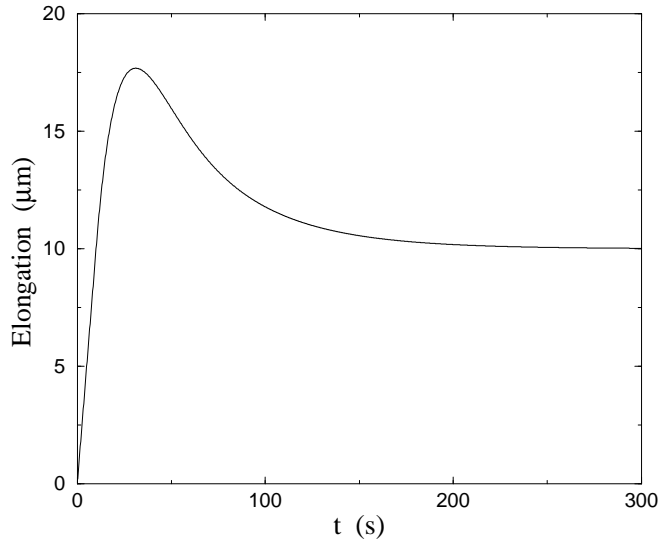


FIG. 8. Steady sliding regime, for the wet case. $\beta = \frac{\nu R}{\eta}$. ($\nu = 10000Kgs^{-1}$, $\eta = 100s$, $m = 10g$, $R = 100\mu m$, $z_m = 10\mu m$, $\beta = \frac{\nu R}{\eta}$, $k = 100Nm^{-1}$, $V = 1\mu ms^{-1}$).

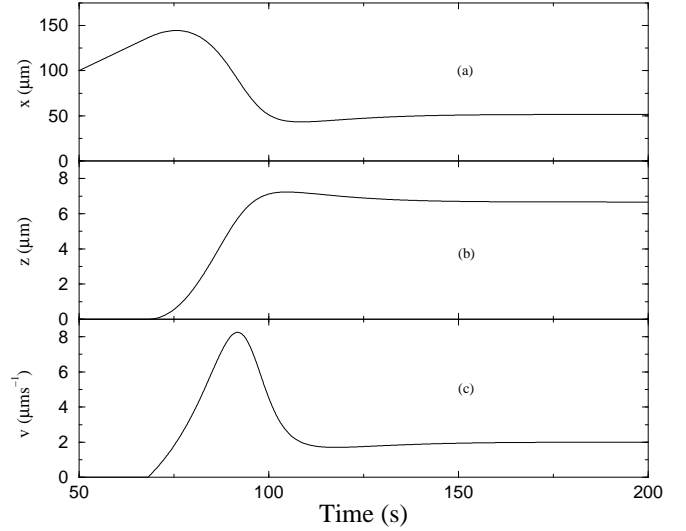


FIG. 9. Steady sliding regime, effect due to $\beta > \frac{\nu R}{\eta}$. ($\nu = 10000Kgs^{-1}$, $\eta = 100s$, $m = 10g$, $R = 100\mu m$, $z_m = 10\mu m$, $\beta = 15\frac{\nu R}{\eta}$, $V = 2\mu ms^{-1}$, $k = 110Nm^{-1}$). (a) spring elongation, (b) horizontal position, (c) plate velocity. With $\beta = 0$ and $\eta \gg 1$ we recover the result of Ref.[4].

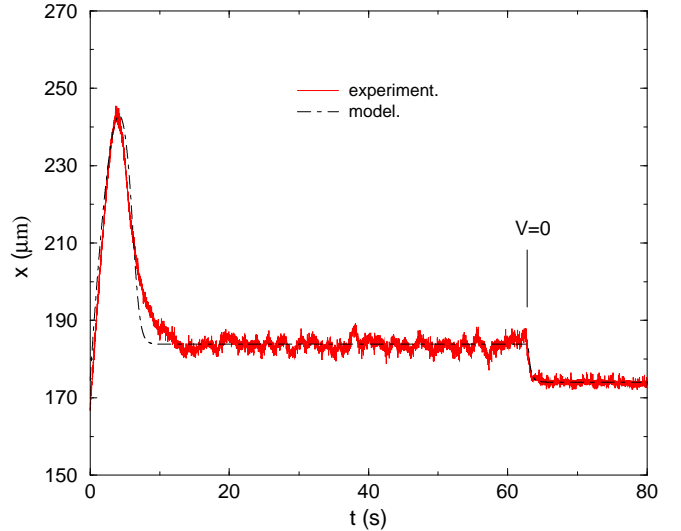


FIG. 10. The plate is stopped in the steady sliding regime (at time $t \approx 60s$) keeping the applied stress constant. We compare the solution of the model with the experimental data of Ref.[4]. ($\nu = 10000Kgs^{-1}$, $\eta = 30s$, $m = 14.5g$, $R = 59\mu m$, $z_m = 6\mu m$, $\beta = 0.01\frac{\nu R}{\eta}$, $V = 28.35\mu ms^{-1}$, $k = 189.5Nm^{-1}$, $A = 0.137\mu mN^{-1}$).

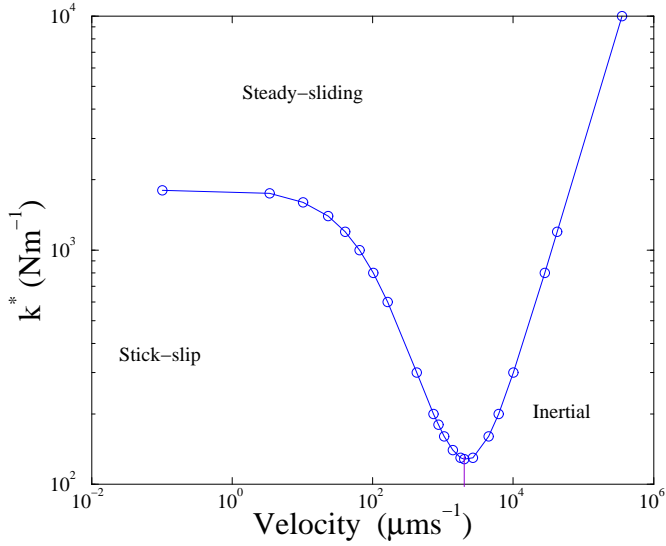


FIG. 11. Dynamical phase diagram. Parameters here have been chosen in order to reproduce the data of Ref.[3]. on dry granular media, the circles are the results of numerical calculation. ($\nu = 90Kgs^{-1}$, $\eta = 0.1s$, $m = 11.3g$, $R = 8\mu m$, $z_m = 8\mu m$, $\beta = 3\frac{\nu R}{\eta}$). We can identify three different zones. At low velocity and low k the system exhibits a stick-slip instability, while at high velocity we observe an inertial regime. We also observe an intermediate region characterized by steady sliding.

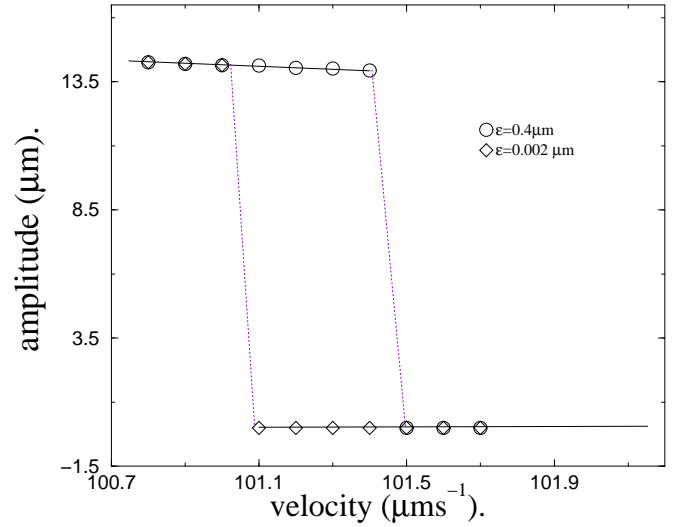


FIG. 13. Amplitude of the oscillation as a function of driving velocity. We perturb the system near its fixed point in the vertical direction. Two amplitudes are used in order to identify the three regimes, the diagram represents the final state of the system as a function of the perturbation ϵ . ($\nu = 90Kgs^{-1}$, $\eta = 0.1s$, $m = 10g$, $R = 8\mu m$, $z_m = 8\mu m$, $\beta = 3\frac{\nu R}{\eta}$, $k = 800Nm^{-1}$).

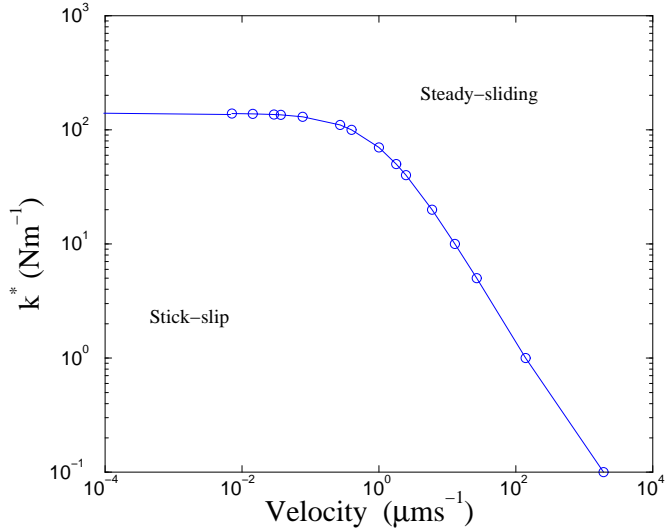


FIG. 12. Dynamical phase diagram for parameters corresponding to the wet case. At high V and k we have a steady-sliding phase which becomes unstable at $k = k^*$. ($\nu = 10000Kgs^{-1}$, $\eta = 100s$, $m = 10g$, $R = 100\mu m$, $z_m = 10\mu m$, $\beta = 15\frac{\nu R}{\eta}$). The circles represent numerical calculation.